

Nonrigid registration of brain MRI using NURBS

Jianzhe Wang, Tianzi Jiang *

National Laboratory of Pattern Recognition, Institute of Automation, Chinese Academy of Sciences, 95 Zhong Guan Cun East Road, Beijing 100080, PR China

Received 11 January 2005; received in revised form 21 September 2005
Available online 1 September 2006

Communicated by C.-F. Westin

Abstract

The focus of medical image registration has shifted to nonrigid registration. It is also a core component in computational neuroanatomy. In this paper, we propose an efficient registration framework which has feature of multiresolution and multigrid. In contrast to the existing registration algorithms. Free-Form Deformations based NURBS (Nonuniform Rational *B* Spline) are used to acquire nonrigid transformation. This can provide a competitive alternative to Free-Form Deformations based *B* spline on flexibility and accuracy. To our knowledge, it is the first report of the use of this mathematical tool for medical image registration. Subdivision of NURBS is extended to 3D and is used in hierarchical optimization to speed up the registration and avoid local minima. The performance of this method is numerically evaluated on simulated images and real images. Compared with the registration method using uniform Free-Form Deformations based *B* spline, our method can successfully register images with improved performance.

© 2006 Elsevier B.V. All rights reserved.

Keywords: Nonrigid registration; Free-Form Deformations; NURBS

1. Introduction

Image registration is the process of estimating an optimal transformation between two images, which is often an essential step in automated medical image analysis. A rigid registration is composed solely of a rotation and translation preserves the “rigid” body constraint. This type of registration is distance preserving and is adequate for many applications in medical image including multimodality and intrasubject registration. However, for intersubject registration or atlas matching, nonrigid algorithms are required. In a nonrigid approach, the “rigid” body constraint is no longer acceptable as it does not account for the nonlinear morphometric variability between subjects, i.e. there exists inherent anatomical variations between different individuals resulting in brain structures that vary in both size and shape. Nonrigid registration algorithms allow

one image to deform to match another image, thus overcoming local variations. In contrast to rigid registration, nonrigid registration algorithms are still the subject of significant ongoing research activity.

Nonrigid registration of medical images has been studied in numerous works in the last decade (Hajnal et al., 2001, Maintz and Viergever, 1998), and various approaches have been proposed to solve this problem. In these methods, FFD (Free-Form Deformations) has been shown to be a valuable tool in medical image registration (Soza et al., 2002, Otte, 2001, Rueckert et al., 1999, Schnabel et al., 2001, Rohlfing et al., 2003). The idea of the FFD is simple: by embedding the object to be deformed in a simple, yet flexible, solid, the deformation of the solid is propagated to the embedded object. In (Soza et al., 2002, Otte, 2001), Bernstein basis functions were used to express deformation. However, Bernstein basis functions have no strict local support, which leads to large computational complexity and insufficient deformation. In (Rueckert et al., 1999, Schnabel et al., 2001, Rohlfing et al., 2003), a FFD based

* Corresponding author. Tel.: +86 10 8261 4469; fax: +86 10 6255 1993.
E-mail address: jiangtz@nlpr.ia.ac.cn (T. Jiang).

B spline for MRI registration was proposed. B spline basis functions have strict local support and better flexibility. That is, a change of control point affects the transformation only in a local neighborhood of that control point. The method works well in most cases, but we found this method has some disadvantages. Because of modelling the transformation with a linear combination of cubic B spline placed on a regular grid, it strictly restricts the parametric solid to a regular parallelepiped with uniform division. This will reduce the flexibility of the method. That is, useful registration points that lie between nodes may be missed, which results in a misregistration.

In contrast to intrasubject registration, the motivation for the use of nonrigid matching in intersubject registration is quite different. Here, the aim of nonrigid registration is to account for the variability of these structures across different individuals rather than to account for the physical deformation of the underlying anatomical structures. Low dimensional and small deformation image registration algorithms can only determine correspondences between images at a coarse global level. High dimensional large deformation image registration algorithms are needed to describe the complex shape differences between individuals.

As a result, the transformation used for intersubject registration must have a larger number of degrees of freedom and are less tightly constrained than those used for intrasubject registration. [Hellier et al. \(2003\)](#) demonstrated that the quality of the registration is directly related to the transformation's degrees of freedom. Thus it is necessary to develop more powerful alternative to the existing registration algorithms. In order to get more flexibility and accuracy, we introduce a new approach to nonrigid registration of brain MRI images. The main contributions of the proposed method can be outlined as follows. First, uniform B spline basis functions are replaced by NURBS during registration because NURBS can allow nonuniform distribution of control points and knot vectors. Second, subdivision of NURBS curve was extended to 3D solid and used in multilevel optimization to avoid local minima and improve accuracy. In addition, in order to prevent the optimization process from producing transformations that are physically incorrect, we also introduce a new constraint scheme that allows us to regularize transformations that are topologically correct. All these merits lead to a substantial increase in computational efficiency.

The rest of this paper is organized as follows. Section 2 describes our new nonrigid registration algorithms in detail, including rigid registration, the theory of FFD transformations, initializing control points, regularization, multiresolution and multigrid, and optimization. In Section 3, in order to evaluate our registration algorithm, we apply it on synthetic and real MRI. Then the results obtained by the new method are compared with registration result that used B spline registration method. Finally, Section 4 summarizes the paper with some conclusions.

2. Methods

Nonrigid registration method can be described with three components: a transformation which relates the floating image and reference image, a similarity measure which measures the similarity between the floating image and reference image, and an optimization which determines the optimal transformation parameters as a function of the similarity measure. Given two input images, floating image $I_f(\mathbf{x})$ and reference image $I_r(\mathbf{x})$, the goal of nonrigid registration is to generate a mapping relating $I_f(\mathbf{x})$ to $I_r(\mathbf{x})$, where $\mathbf{x} = [x, y, z]^T$ is any point location in the images. Then registering images $I_f(\mathbf{x})$ and $I_r(\mathbf{x})$ is equivalent to finding the displacement fields $\mathbf{d}(\mathbf{x})$ such that $\mathbf{x} + \mathbf{d}(\mathbf{x})$ is a one to one onto continuous map and for which cost function $F(I_r(\mathbf{x}), I_f(\mathbf{x} + \mathbf{d}(\mathbf{x})))$ is optimized. The cost function contains terms $C_{\text{similarity}}$ that measure how well images $I_f(\mathbf{x})$ and $I_r(\mathbf{x})$ are aligned and also have regularization terms $C_{\text{regularization}}$ that impose restrictions on transformation. In general, the regularization on the transformation preserve the natural topology of the image, impeding the transformation from producing artifacts known as “folding” and “tearing” of the image.

Traditionally, a rigid or affine global registration is required before nonrigid registration, which will align images globally. Nonrigid registration then corrects local elastic deformation. In this study, we will also follow this procedure: rigid registration is briefly described in Section 2.1, and then our nonrigid registration method with NURBS is described in detail in Section 2.2.

2.1. Rigid registration

The goal of rigid registration is to find six degrees of freedom (three rotations and three translations). Mutual information was introduced for medical image registration by [Collignon et al. \(1995\)](#), and by [Viola and Wells \(1995\)](#), which can qualitatively be thought of as a measure of how well one image explains the other and is maximized at the optimal alignment. Since no assumption is made regarding the nature of the relation between the image intensities in both images, it is powerful and general, and can be applied automatically without any assumption. Because the joint histogram, and therefore the probability distributions, are computed only for the overlapping part of the images, the mutual information measure is dependent on the overlap. To overcome this, Normalized Mutual Information (NMI) ([Studholme et al., 1999](#)) has been proposed, which prevents the actual amount of image overlap to affect the measure. Therefore, we will use NMI as similarity measure in this paper.

$$C_{\text{similarity}} = \frac{H(I_r(\mathbf{x})) + H(I_f(\mathbf{x}))}{H(I_r(\mathbf{x}), I_f(\mathbf{x}))} \quad (1)$$

where $H(I_r(\mathbf{x}))$ and $H(I_f(\mathbf{x}))$ are the marginal entropies of images $I_r(\mathbf{x})$, $I_f(\mathbf{x})$, and $H(I_r(\mathbf{x}), I_f(\mathbf{x}))$ is their joint entropy,

which is calculated from the joint histogram of $I_1(\mathbf{x})$ and $I_2(\mathbf{x})$.

Our rigid registration algorithm is based on an independent implementation of a technique described in (Maes et al., 1997). The method is employed directly for finding an initial rigid transformation to capture the global displacement of both images. Thus the rigid transformation is used as the initial estimate for the nonrigid registration.

2.2. Nonrigid registration

In this subsection, we first give an introduction to theory of Free-Form Deformation and NURBS. Then we detail our methodology for nonrigid registration of brain MRI.

2.2.1. Free-Form Deformation with NURBS

FFD allows the user conceptually embed an object into a clear pliable solid and apply deformation to the solid, they then carry through to the encased object. In (Rueckert et al., 1999), the deformation function is defined on a uniformly spaced grid of control points $P_{i,j,k}$. At any position x , the deformation is computed from the positions of the surrounding $4 \times 4 \times 4$ neighborhood of control points

$$D(x) = \sum_{i=0}^3 \sum_{j=0}^3 \sum_{k=0}^3 B_i(u)B_j(v)B_k(w)P_{i+j+k,n} \quad (2)$$

where, i, j and k denote the index of the control point cell containing x , u, v and w are the relative positions of x in the three dimensions. The functions B is cubic uniform B spline basis function.

$$\begin{aligned} B_0(t) &= (-t^3 + 3t^2 - 3t + 1)/6 \\ B_1(t) &= (3t^3 - 6t^2 + 4)/6 \\ B_2(t) &= (-3t^3 + 3t^2 + 3t + 1)/6 \\ B_3(t) &= t^3/6 \end{aligned} \quad (3)$$

Although this method works well in most cases, it fails to register some images, especially when there are large difference between the two images (refer to Hartkens et al., 2002 for more information).

The main motivation of this paper is to address the above mentioned problem with uniform B spline. We find that NURBS (Piegl and Tiller, 1997) can satisfy above requirements. NURBS generalizes the nonrational parametric form. They are infinitely smooth in the interior of a knot span provided the denominator is not zero, which enables them to satisfy different smoothness requirements. Moreover, they have some additional properties:

- NURBS include weights as extra degrees of freedom which influence local shape. The spline is attracted toward a control point more if the corresponding weight is increased and less if the weight is decreased, which can be seen in Fig. 1, increased weight pulls the curve toward control point P_3 .

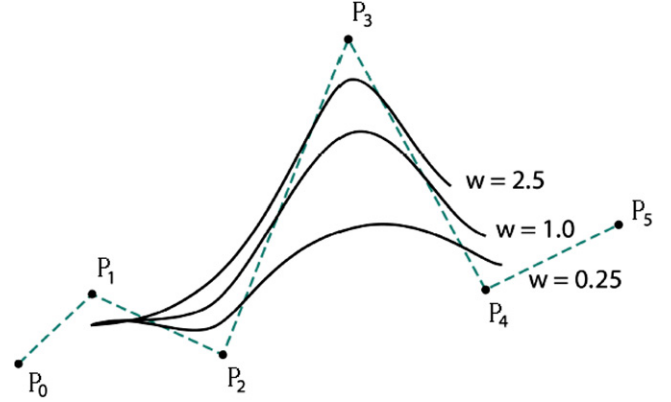


Fig. 1. Increased weight pulls the curve toward control point P_3 .

- NURBS offer a common mathematical framework for implicit and parametric polynomial forms. This powerful modelling flexibility is achieved through the specific combinations of control points, weights.

Since the knot vectors and control points are no longer constrained to a regular initial spacing. It is helpful to develop an FFD with NURBS for image registration. NURBS is integrated into FFD, then the hyperpatch can be expressed as

$$D(x) = \frac{\sum_{i=0}^p \sum_{j=0}^q \sum_{k=0}^r B_{i,l}(u)B_{j,m}(v)B_{k,n}(w)W_{i,j,k}P_{i,j,k}}{\sum_{i=0}^p \sum_{j=0}^q \sum_{k=0}^r B_{i,l}(u)B_{j,m}(v)B_{k,n}(w)W_{i,j,k}} \quad (4)$$

where $B_{i,l}$, $B_{j,m}$ and $B_{k,n}$ represent the l th, m th and n th B spline basis functions respectively, and can be calculated by DeBoor–Cox iteration (DeBoor, 1972). p, q, r are the number of divisions through three orthogonal directions within the control points. Each control point $P_{i,j,k}$ have an associated number called weight $W_{i,j,k}$.

As mentioned above, changing the weight $W_{i,j,k}$ of a control point $P_{i,j,k}$ affects only the range $\{(u_i, u_{i+l+1}), (v_j, v_{j+m+1}), (w_k, w_{k+n+1})\}$. Between moving control points and adjusting their weights, NURBS provide a much more flexible tool than uniform B spline. It is interesting to point out that (4) is identical with (2) when $W_{i,j,k}$ is set to unity and knot vectors are uniform. Therefore, the FFD based uniform B spline is a special case of the FFD based NURBS.

In our approach we do not consider the absolute coordinates of the control points for obtaining the deformations field directly. If control points move from the initial positions to new locations with displacement ΔP , then using formulation (4), we can derive the displacement field of every point within the lattices:

$$d(x) = \frac{\sum_{i=0}^p \sum_{j=0}^q \sum_{k=0}^r B_{i,l}(u)B_{j,m}(v)B_{k,n}(w)W_{i,j,k}\Delta P}{\sum_{i=0}^p \sum_{j=0}^q \sum_{k=0}^r B_{i,l}(u)B_{j,m}(v)B_{k,n}(w)W_{i,j,k}} \quad (5)$$

2.2.2. Initializing control points

In (Rueckert et al., 1999, Rohlfing et al., 2003), control points were placed regularly, so there are many control points placed in background areas where there is little information to help the registration. Moreover, it is not necessary to estimate the pointwise correspondence for all voxels in a image, but only within the object or region-of interest (ROI). For example, when registering brain images, we only care about the correspondence within the brain and do not care about correspondences outside the brain. We made the following assumption. The corner region of MRI (not the corner of brain) is usually background, and maintains unchanged during registration. Moreover, difference of brain is possibly large between different subjects. Therefore, it may be desirable to have a nonuniform spacing of control points, they can be coarse in areas requiring little or no deformation and dense in areas requiring abundant deformation. The control points can be divided into an arbitrary number of sections in each of the three orthogonal directions according to property of NURBS.

As previously stated, we hope to initialize control points according to content of image. First, segmentation of background of two images is needed. It is important to note that the quality of the segmentation does not need to be perfect, as the target is just to provide an initial estimate of the background between images $I_r(x)$ and $I_t(x)$. We use the segmented backgrounds as masks. Then control points are placed on the image $I_t(x)$ according to the two masks. That is, there are coarse control points in corner region of MRI. Knot vectors are arranged accordingly. The weight $W_{i,j,k}$ is originally set to unity whilst initializing control points.

2.2.3. Multiresolution method and multigrid framework

If the spacing of control points is large, i.e. the parameter of transformation is not enough, transformation will not provide sufficient deformation in local region. This affects the accuracy of registration result. In order to improve accuracy and avoid local minima, multiresolution method and multigrid framework are used. In this context, resolution means the spatial resolution of the image while the grid is related to the control points in transformation. Inserting some new control points can provide sufficient deformation. It is important to note that knot insertion is really just a change of knot space basis, the shape does not change geometrically.

For cubic NURBS curves as shown in Fig. 2, given knot vector $U = [u_0, u_1, \dots, u_{n+4}]$, the new knot vector $U' = [u'_0, u'_1, \dots, u'_{n+3}]$:

$$u'_i = \frac{u_i + u_{i+1}}{2} \quad (6)$$

Then the elements of U' are to be inserted into U , the corresponding new control points P' is to be computed by new knot vectors and original control points (Piegl and Tiller,

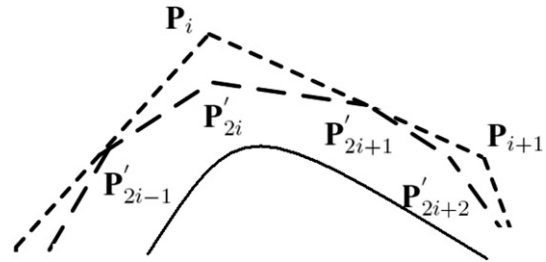


Fig. 2. Cubic NURBS curve subdivision. P is original control points, P' is the new control points.

1997). Clearly, knot refinement can be accomplished by multiple application of knot insertion.

After knot refinement, the resulting control polygon has about twice as many as original control points. It is appreciated that the curve ideas could give surface and solid just by applying the concept of tensor. So we extend it to 3D solid. Refinement of the control point by a factor of 2 per dimension increases the number of control points by roughly a factor of 8. This leads to a dramatic increase in computation time. Our goal is to increase the number of control points selectively in regions where they are needed rather than increase them globally everywhere in the image.

In order to reduce the number of degrees of freedom of the nonrigid transformation, some adaptive grid registrations methods have been proposed. Schnabel et al. (2001) introduced a control point status S associated with each control point, marking it as either active or passive. Active control points are allowed to move during the registration process, whereas passive control points remain fixed. Rohde et al. (2003) used the gradient of global MI to refine grids. Rohlfing et al. (2003) utilized methods based on entropies. Park and Meyer (2003) proposed one local mismatch measure and show that it can have better sensitivity to deformation than the global measure. In this paper, we also use the local mismatch measure M as defined in (Park and Meyer, 2003).

$$M = 1 - \frac{MI(a, b)}{\min(H(a), H(b))} \quad (7)$$

where $MI(a, b)$, $H(a)$ and $H(b)$ are local measures, i.e., they are computed over a finite subregion, not over the whole image. In this paper, we set the subregion size $40 \times 40 \times 40$. Noting that the effects of control points are fairly local, a good candidate region is the region with the largest local mismatch. According the local mismatch measure M , we can exclude some control points from computations.

Because of using multiresolution method and multigrid framework, registration is then achieved by deforming a sequence of control point of increasing resolution using multigrid. The deformation of each point in the image is given by the sum of the local deformations across levels:

$$D(\mathbf{x}) = \mathbf{x} + \sum_{i=1}^N d_i(\mathbf{x}) \quad (8)$$

where $d_i(\mathbf{x})$ is local displacement field on level i , as defined in (5), N is the total number of levels.

2.2.4. Regularization scheme

A common weakness for all forms of spatial deformation is a possible self-intersection or folding of an object (Gain and Dodgson, 2001). The high dimensional transformations involved in nonrigid registration generally make the problem ill-conditioned, so that additional regularization is needed to obtain a satisfactory result.

Previous attempts at constraining spline-based deformation models to produce consistent topological deformations can be found in (Otte, 2001, Rueckert et al., 1999, Schnabel et al., 2001), where the basic idea is to optimize the similarity measure while regularizing the displacement fields by minimizing its second derivative. While this technique can reduce folding artifacts, it can not guarantee the positive definiteness of the Jacobian of the transformation. On the other hand, Rohlfing et al. (2003) used a novel regularization term, i.e., a local volume-preservation (incompressibility) constraint. The incompressibility constraint is implemented by penalizing the Jacobian determinant of the deformation from unity. But the incompressibility regularization term is strictly constrained, which may reduce the flexibility of the method. Moreover, incompressibility that is well suited to intrasubject registration may not be suitable for intersubject registration. Rohde et al. (2003) studied relation of the deformation field and topology, and derive bounds for coefficients of the basis functions. Following it, we introduce a regularization scheme that can be applied explicitly to our deformation function.

For FFD function $D(\mathbf{x})$ in (8), $J(\mathbf{x})$ be the Jacobian matrix of $D(\mathbf{x})$.

$$J(\mathbf{x}) = \begin{bmatrix} \frac{\partial D_x}{\partial x} & \frac{\partial D_x}{\partial y} & \frac{\partial D_x}{\partial z} \\ \frac{\partial D_y}{\partial x} & \frac{\partial D_y}{\partial y} & \frac{\partial D_y}{\partial z} \\ \frac{\partial D_z}{\partial x} & \frac{\partial D_z}{\partial y} & \frac{\partial D_z}{\partial z} \end{bmatrix} \quad (9)$$

Gain and Dodgson (2001) proved that: Let $D(\mathbf{x})$ be a spatial deformation function and $J(\mathbf{x})$ be its Jacobian matrix, $D(\mathbf{x})$ is homeomorphic (injective, onto, and invertible), if

- $D(\mathbf{x})$ has continuous partial derivatives of the first order.
- $\det(J(\mathbf{x})) > 0$.

The first condition can be satisfied if the NURBS basis functions are at least C^2 continuous. The second condition relies on the positivity of the Jacobian, the Jacobian at a point provides a measure of the local distortion. In (Ashburner et al., 1999), they suggested that it was helpful to use the Jacobian determinant as regularization. Consider

$D(\mathbf{x})$, which is the sum of displacement fields at different level, we then obtain the Jacobian matrix of $D(\mathbf{x})$:

$$J(\mathbf{x}) = \mathbf{I} + \sum_{i=1}^N J_i(\mathbf{x}) \quad (10)$$

where \mathbf{I} is the identity matrix, and $J_i(\mathbf{x})$ is the Jacobian matrix of the displacement field $d_i(\mathbf{x})$. In (Rohde et al., 2003), they prove that if the constraint

$$\|J_{N+1}(\mathbf{x})\|_2 < 1 - \left\| \sum_{i=1}^N J_i(\mathbf{x}) \right\|_2 \quad (11)$$

is satisfied, then the Jacobian remains positive.

Using the well known triangle inequality $\left\| \sum_{i=1}^N J_i(\mathbf{x}) \right\|_2 \leq \sum_{i=1}^N \|J_i(\mathbf{x})\|_2$, we then obtain

$$\|J_{N+1}(\mathbf{x})\|_2 < 1 - \sum_{i=1}^N \|J_i(\mathbf{x})\|_2 \quad (12)$$

Here, it is a tight condition for $J_{N+1}(\mathbf{x})$. After optimization on each level, we can save $J_i(\mathbf{x})$ and use it to derive the bound for $J_{N+1}(\mathbf{x})$. In contrast to condition (11), computation of this condition is expedient.

For a given deformation field $d_i(\mathbf{x})$, a new displacement field $d_{i+1}(\mathbf{x})$ can be added without violating the topology constraint as long as relationship (12) is satisfied.

2.2.5. Optimization

As stated above, based on the regularization, we can prevent the optimization process from producing transformations that are physically incorrect. In order to find the optimal transformation, the main idea of the nonrigid registration is to manipulate control points and weights in such a way that $I_t(\mathbf{x})$ aligns with $I_r(\mathbf{x})$. The cost function is defined:

$$F_{\text{cost}} = -C_{\text{similarity}} \quad (13)$$

Here, the term $C_{\text{similarity}}$ is the NMI between images $I_r(\mathbf{x})$ and $I_t(D(\mathbf{x}))$, although the approach we propose is not limited to this particular similarity measure. In our implementation, the NMI value is always evaluated over all the voxels belonging to the overlapping domain of images $I_r(\mathbf{x})$ and $I_t(D(\mathbf{x}))$.

Modified Powell's direction set method is used because it is efficient to carry out local search. At every iteration, a coordinate in one dimension of only one control point is changed, and the new volume obtained with FFD is computed. We check relationship (12) to guarantees topological correctness. then compute the NMI value between $I_r(\mathbf{x})$ and $I_t(D(\mathbf{x}))$. The procedure repeats until the NMI value reaches its optimum. After optimization of the control point, we turn to the weight associated with the control point, which can be seen as the fourth component of the control point. With the subdivision of the control points, the image resolution increases from coarse to fine, optimization runs on each level one by one. A flowchart of the proposed algorithm is shown in Fig. 3.

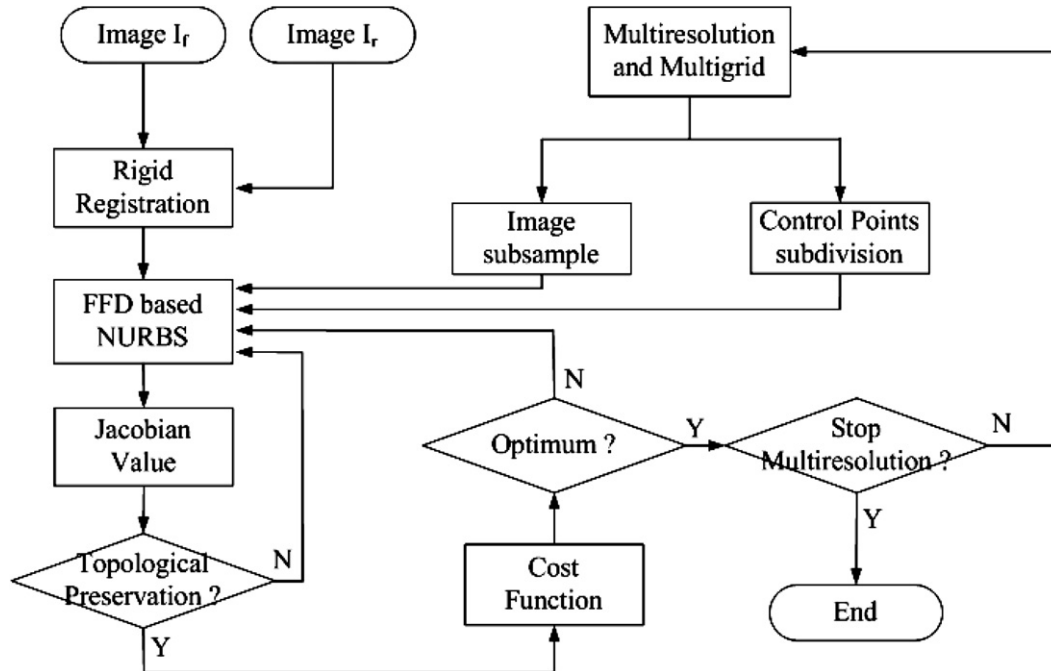


Fig. 3. The FFD based NURBS registration algorithm.

3. Experimental results

We describe two experiments to demonstrate the performance of our registration algorithm. The first experiment depicts the procedure for recovering a known deformation, the experiment also demonstrates the ability of our model to cope with multimodal images. The second experiment provides a validation of our algorithm on 14 subjects. The purpose of these experiments is to demonstrate that our method can achieve an efficient and accurate registration on various images with very large deformation as well as small deformation. Control points are set to three levels in these experiments, and the initiatory control points are shown in Table 1. Also, the images were subsampled with a factor of 2, and resulting in image with 2- and 4-mm isotropic voxels. We have done a comparison between our FFD based NURBS registration method (NFFD) and the FFD based uniform B spline registration method (FFD).

3.1. Experiments on synthetic datasets

A T1 weighted image of MNI (www.bic.mni.mcgill.ca/brainweb) is used in the experiment. The image have

$181 \times 217 \times 181$ voxels of size $1 \times 1 \times 1 \text{ mm}^3$. In the ideal case, the accuracy of our algorithm in registering volumes should be tested in a situation that the actual motion is known. Due to the difficulty to produce known nonrigid motion fields in biological tissues of brain, we have created five artificially deformed volume by applying known warps, which were designed using thin plate splines (Bookstein, 1989) on the volume. These simulated deformation volumes have been chosen as a reference images respectively. One registration results are displayed in Fig. 4. As a qualitative measure, we have chosen to use the difference image between the result image and the reference image. We can see that our method achieved better result than FFD method, expressly in up-left edge of image, the amount of misregistration visibly reduced significantly. The difference image is almost zero everywhere except at a few sparse locations.

For a quantitative evaluation, 100 random positions are selected in the floating image for each warp, and their corresponding positions in reference image are acquired from these five known warps. We compute the deformed position of these points and compare them to the corresponding points in the reference image. Table 2 summarizes the registration quality in terms of correlation coefficient (CC) and normalized mutual information (NMI), and Table 3 summarizes mean error and maximal error between true and recovered deformation for the registration in these five warps, which are our selected indicator of the quality of the registration. The results clearly show that NFFD improves the correlation.

We also test the algorithm on multimodal image. We utilize one artificially deformed T1 weighted image as floating

Table 1
Initialization of control points

	Experiment 1	Experiment 2
Band	9	10
Row	10	12
Column	9	12

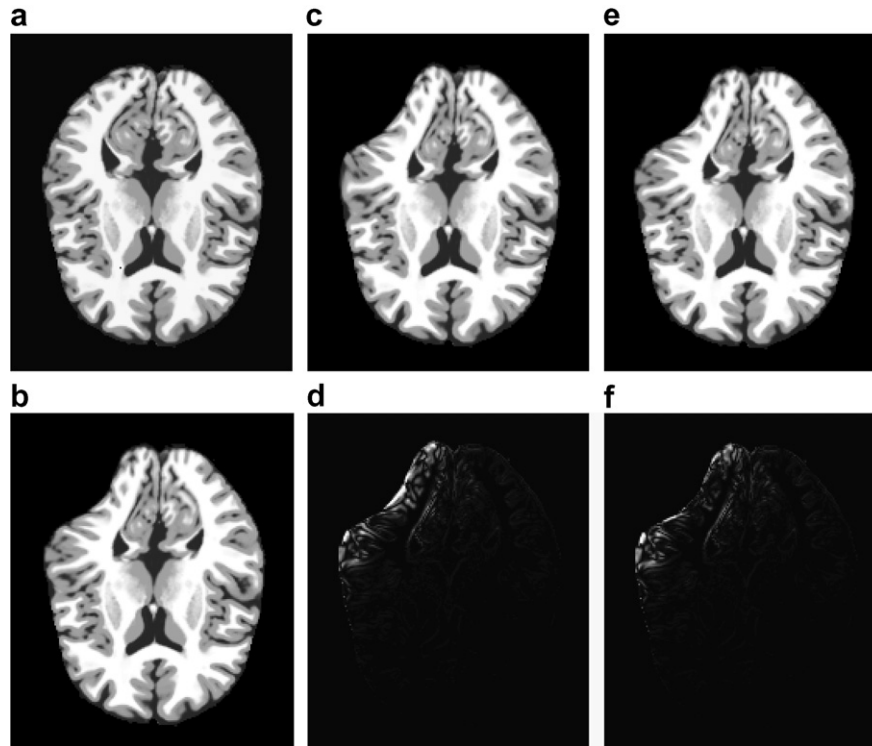


Fig. 4. Registration results on synthetic images. (a) Floating image, (b) reference image to be registered, (c) the registration result using FFD, (d) difference image between (b) and (c), (e) registration result using NFFD, (f) difference image between (b) and (e).

Table 2
CC and NMI values

Warp	CC		NMI	
	NFFD	FFD	NFFD	FFD
1	0.97875	0.94454	1.245	1.204
2	0.97007	0.93797	1.237	1.223
3	0.98754	0.94879	1.312	1.287
4	0.98478	0.95875	1.244	1.241
5	0.98587	0.95417	1.328	1.314

Table 3
Mean error and maximal error

Warp	Mean error		Maximal error	
	NFFD	FFD	NFFD	FFD
1	0.35	0.37	1.47	1.62
2	0.33	0.42	1.03	1.07
3	0.31	0.34	1.33	1.38
4	0.25	0.26	0.85	1.15
5	0.37	0.39	1.61	1.76

image. The T2 weighted image of MNI is selected as reference image. Fig. 5 shows the registration results. (a) and (b) depict the floating and reference images to be registered. (c) depicts the result after FFD and the result using NFFD is shown in (d). Large difference are still visible after FFD registration, for instance, distortions are clearly visible on the ventricles, the misalignment has been dramatically reduced after the application of our method. For multi-modal image, we only compare the NMI value after regis-

tration. The value after FFD is 1.175, while it is 1.214 for the NFFD.

3.2. Experiments on datasets of 14 subjects

In this study we evaluate the performance of NFFD on 14 different subjects. The MR brain images were obtained with high-resolution 3D SPGR pulse sequences (FOV 24×24 cm, 256×256 , 1.5 mm thickness, 0 mm gap, TE = 1.9 ms, flip angle = 20° , T1 = 450 ms, TR = 11.9 ms). Before performing the intersubject registration, all images have been stripped of extracranial tissue by MRIcro. The stripping of extracranial tissue removes the influence of extracranial structures like skin and bone on the registration results. Moreover, in order to facilitate further processing, analysis and visualization tasks, it is advantageous to have voxel dimensions which are isotropic. Thus the brain images were resampled to $200 \times 200 \times 176$ with 1.0 mm^3 voxels.

Here, we chose one subject as the reference subject, then perform the registration between the reference and the other 13 subjects (floating). Finally, we obtained 13 registered volumes. As in experiment 1, we compare the NMI values, which can be seen in Fig. 6. It shows that NFFD is more accurate than the FFD approach. The average final NMI values for the registrations which used FFD was 1.282, while it is 1.301 for the NFFD approach.

Fig. 7 depicts one registration result. The contours of the reference image were overlaid on the images as a

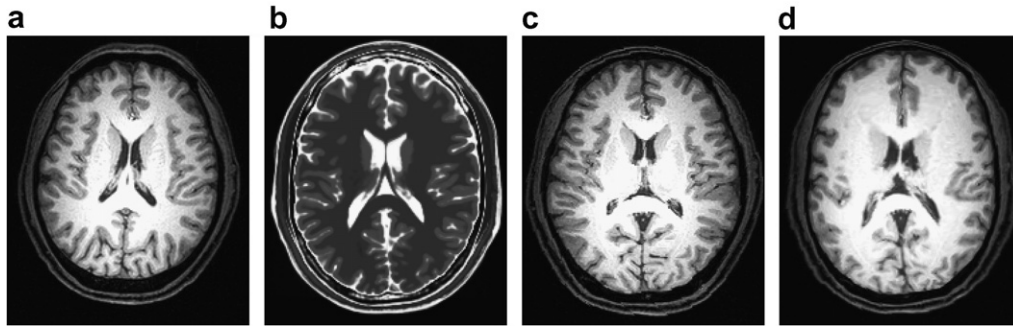


Fig. 5. Registration on multimodal images. (a) Floating image, (b) reference image to be registered, (c) the registration result using FFD, (d) registration result using NFFD.

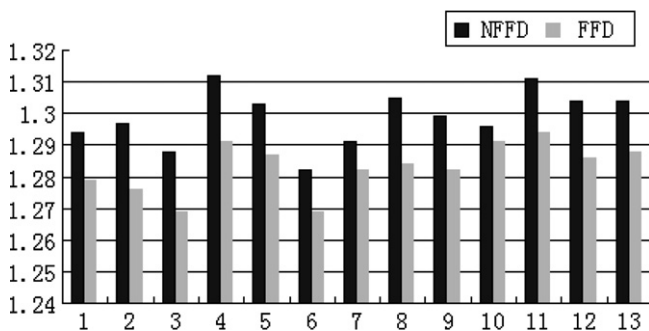


Fig. 6. Comparison of the registration in term of NMI values.

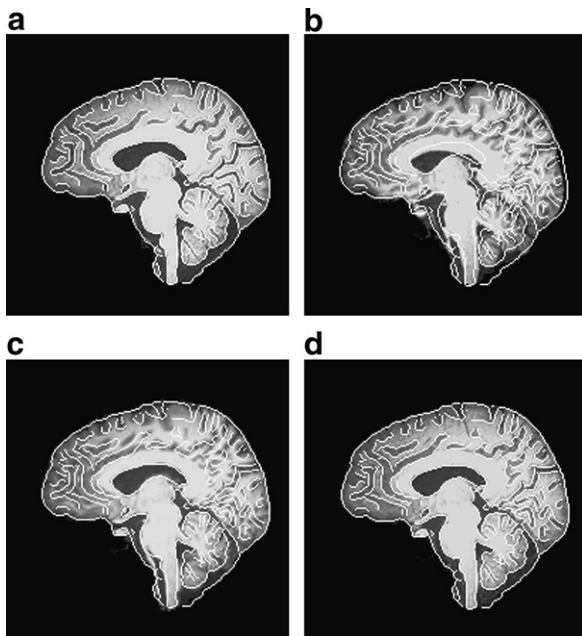


Fig. 7. Registration results on real images, contours of the reference image (white line) were overlaid on the resulting images as a reference of registration accuracy. (a) Reference image, (b) result image using affine registration, (c) result image using FFD registration, (d) result image using NFFD registration.

reference of registration accuracy. The results demonstrate that FFD and NFFD lead to a significantly improved contrast against affine, for example, both algorithms align the

ventricular system well. But some deviations can be observed in Fig. 7(c), NFFD yields better results, this can be seen on white matter tracks, and even cortical regions. We observe that it is difficult to do any meaningful comparison of the volumes prior to registration. However, once the registration is performed, even small differences are apparent. Moreover, the deformation itself can provide valuable quantitative information about the relative sizes and shapes between floating image and reference image, which greatly facilitate further analysis, such as: deformation based morphometry (Ashburner et al., 2003).

On the other hand, one straightforward way to assess the quality of the registration is to evaluate how the tissues are deformed from one subject to the other, we therefore evaluate the registration quality by computing the overlap between the tissues of the reference image and the tissues of each floating image after registration. The extraction of white matter, gray matter and cerebral spinal fluid is performed using our previous technique (Zhu and Jiang, 2003). In this segmentation algorithm, multicontext fuzzy clustering (MCFC) is proposed for classifying MR data into tissues of white matter, gray matter, and cerebral spinal fluid automatically. We then used warping of the labeled reference image to obtain a fully automated labeling of 13 subjects. The performances of two registration methods were then compared by using overlap coefficients for white matter, gray matter and cerebral spinal fluid, and the results are presented in Table 4. Affine registration performs worst in this study as we expect, the results obtained with FFD and NFFD are comparable. However, the NFFD consistently improves the registration quality, i.e., after FFD registration, for grey matter tissue, the average overlap is 83.71%, but it is 91.27% for NFFD.

Table 4

Average overlap coefficients (in %) for different tissue classes after affine, FFD and NFFD registration

	Affine	FFD	NFFD
Gray matter	67.27	83.71	91.27
White matter	71.68	87.43	90.68
Cerebral spinal fluid	56.44	71.29	80.74

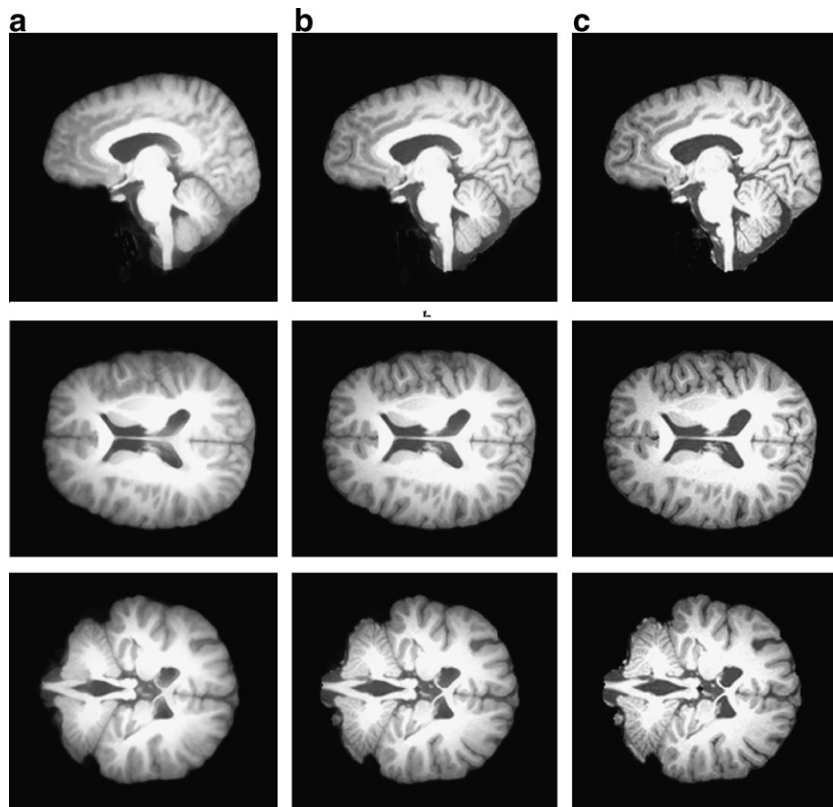


Fig. 8. Average brain image reconstructed from 13 very different subjects in three different views. (a) Average after FFD registration, (b) average after NFFD registration, (c) the reference image.

The sharpness of the average of the warped brain images is often used as a visual display of the accuracy of registration algorithms. We averaged all the registered volume in order to have a global overview of the quality of the method. These are shown in Fig. 8. The average computed after NFFD registration is visibly sharper than the average computed after FFD, indicating that, overall, the new approach succeeded in matching image better than the traditional one. For example, we notice that the internal anatomical structures are blurred, because the registration is not precise enough after FFD registration. However, after NFFD registration, we may distinguish precisely the contours of anatomical structures, such as: ventricles and WM/GM boundaries are very clear.

Finally, a comparison of runtime between NFFD and FFD was performed. Average run time for one patient is about 7 h for NFFD and 6 h for FFD on a Pentium IV 2.4 GHz processor with 1 GB of memory. We can appreciate that, in contrast to FFD, we obtain better registration quality and comparable runtime with NFFD.

4. Conclusions

In this paper, a novel nonrigid registration approach has been proposed. An important aspect of our algorithm is the expression for the nonrigid transformation of image coordinates. We model image deformations on FFD based on NURBS because of their computational efficiency and abil-

ity of local control. Although NURBS is a mature and powerful tool and has been used in various fields, it has never been used in image registration. Our experimental results show that NURBS is also a powerful tool for nonrigid registration. In comparison to the existing counterparts, the NFFD has more flexibility. Also, we introduce a regularization scheme, which guarantees topological correctness. The experimental results show that the proposed method is a promising alternative to the existing methods.

Acknowledgements

This work was partially supported by Hundred Talents Programs of the Chinese Academy of Sciences, the Natural Science Foundation of China, Grant No. 60172056, 60121302, and the National Key Basic Research and Development Program (973) Grant No. 2003CB716104.

References

- Ashburner, J., Andersson, J.L.R., Friston, K.J., 1999. High-dimensional image registration using symmetric priors. *NeuroImage* 9 (6), 619–628.
- Ashburner, J., Hutton, C., Frackowiak, R., Johnsrude, I., Price, C., Friston, K., 2003. Identifying global anatomical differences: Deformation-based morphometry. *Human Brain Map.* 6 (5), 348–357.
- Bookstein, F.L., 1989. Principal warps: Thin-plate splines and the decomposition of deformations. *IEEE Trans. Pattern Anal. Machine Intell.* 11 (6), 567–585.

- Collignon, A., Maes, F., Delaere, D., Vandermeulen, D., Suetens, P., Marchal, G., 1995. Automated multimodality image registration using information theory. In: *Proc. IPMI*, 1995, pp. 263–274.
- Deboor, C., 1972. On calculating with B-splines. *J. Approximat. Theory* 6 (1), 50–62.
- Gain, J., Dodgson, N., 2001. Preventing self-intersection under free-form deformation. *IEEE Trans. Visualization Comput. Graph.* 7 (4), 289–298.
- Hajnal, J.V., Hill, D.L.G., Hawkes, D.J., 2001. *Medical Image Registration*. CRC Press.
- Hartkens, T., Hill, D.L.G., Castellano-Smith, A.D., Hawkes, D.J., Maurer, C.R., Jr., Martin, A.J., Hall, W.A., Liu, H., Truwit, C.L., 2002. Using points and surfaces to improve voxel-based nonrigid registration. In: *Proc. Conf. MICCAI*, pp. 565–572.
- Hellier, P., Barillot, C., Corouge, I., Gibaud, B., Le Goualher, G., Collins, D.L., Evans, A., Malandain, G., Ayache, N., Christensen, G.E., Johnson, H.J., 2003. Retrospective evaluation of intersubject brain registration. *IEEE Trans. Med. Imag.* 22 (9), 1120–1130.
- Maes, F., Collignon, A., Vandermeulen, D., Marchal, G., Suetens, P., 1997. Multimodality image registration by maximization of mutual information. *IEEE Trans. Med. Imag.* 16 (2), 187–198.
- Maintz, J.B., Viergever, M.A., 1998. A survey of medical image registration. *Med. Image Anal.* 2 (1), 1–36.
- Otte, M., 2001. Elastic registration of fMRI data using bezier-spline transformation. *IEEE Trans. Med. Imag.* 20 (2), 187–198.
- Park, H., Meyer, C., 2003. Grid refinement in adaptive non-rigid registration. In: *Proc. Conf. MICCAI*, pp. 796–803.
- Piegl, L., Tiller, W., 1997. *The NURBS Book*. Springer.
- Rohde, G.K., Aldroubi, A., Dawant, B.M., 2003. The adaptive bases algorithm for intensity-based nonrigid image registration. *IEEE Trans. Med. Imag.* 22 (11), 1470–1479.
- Rohlfing, T., Maurer, C.R., Bluemke Jr., D.A., Jacobs, M.A., 2003. Volume-preserving nonrigid registration of MR breast images using free-form deformation with an incompressibility constraint. *IEEE Trans. Med. Imag.* 22 (6), 730–741.
- Rueckert, D., Sonoda, L.I., Hayes, C., Hill, D.L., Leach, M.O., Hawkes, D.J., 1999. Nonrigid registration using free-form deformations: Application to breast MR images. *IEEE Trans. Med. Imag.* 18 (8), 712–721.
- Schnabel, J.A., Rueckert, D., Quist, M., Blackall, J.M., Smith, A.D.C., Hartkens, T., Penney, G.P., Hall, W.A., Liu, H., Truwit, C.L., Gerritsen, F.A., Hill, D.L.G., Hawkes, D.J., 2001. A generic framework for non-rigid registration based on non-uniform multi-level free-form deformations. In: *Proc. Conf. MICCAI*, pp. 573–581.
- Soza, G., Bauer, M., Hastreiter, P., Nimsky, C., Greiner, G., 2002. Nonrigid registration with use of hardware-based 3D bezier functions. In: *Proc. Conf. MICCAI*, pp. 549–556.
- Studholme, C., Hill, D.L.G., Hawkes, D., 1999. An overlap invariant entropy measure of 3D medical image alignment. *Pattern Recognition* 32 (1), 71–86.
- Viola, P., Wells, W.M., 1995. Alignment by maximization of mutual information. In: *Internat. Conf. on Computer Vision*. IEEE Computer Society Press, Los Alamitos, CA, pp. 16–23.
- Zhu, C.Z., Jiang, T.Z., 2003. Multi-context fuzzy clustering for separation of brain tissues in MR images. *NeuroImage* 18 (3), 685–696.